Plant Physiology®

Research Article

Armadillo repeat only protein GS10 negatively regulates brassinosteroid signaling to control rice grain size

Erwang Chen [iD],[1,2,†] Qingqing Hou,[1,3,†] Kun Liu [iD],[1,4,†] Zhoulin Gu [iD],[1] Bingxin Dai [iD],[1,5] Ahong Wang [iD],[1] Qi Feng [iD],[1] Yan Zhao,[1] Congcong Zhou [iD],[1] Jingjie Zhu [iD],[1] Yingying Shangguan,[1] Yongchun Wang [iD],[1] Danfeng Lv [iD],[1] Danlin Fan [iD],[1] Tao Huang [iD],[1] Zixuan Wang [iD],[1] Xuehui Huang [iD][6] and Bin Han [iD][1,*]

1   National Center for Gene Research, CAS Center for Excellence in Molecular Plant Sciences, Institute of Plant Physiology and Ecology, Chinese Academy of Sciences, Shanghai 200233, China
2   Division of Life Sciences and Medicine, School of Life Sciences, University of Science and Technology of China, Chinese Academy of Sciences, Hefei 230027, China
3   State Key Laboratory of Crop Gene Exploration and Utilization in Southwest China, Rice Research Institute, Sichuan Agricultural University at Wenjiang, Chengdu 611130, China
4   College of Life Sciences, Anhui Normal University, Wuhu, Anhui 241000, China
5   School of Life Science and Technology, Shanghai Tech University, Shanghai 201210, China
6   College of Life Sciences, Shanghai Normal University, Shanghai 200234, China

*Author for correspondence: bhan@ncgr.ac.cn
†These authors contributed equally to this work.
The author responsible for distribution of materials integral to the findings presented in this article in accordance with the policy described in the Instructions for Authors (https://academic.oup.com/plphys/pages/General-Instructions) is Bin Han (bhan@ncgr.ac.cn).

Abstract

Grain yield and grain quality are major determinants in modern breeding controlled by many quantitative traits loci (QTLs) in rice (*Oryza sativa*). However, the mechanisms underlying grain shape and quality are poorly understood. Here, we characterize a QTL for grain size and grain quality via map-based cloning from wild rice (W1943), *GS10* (<u>G</u>rain <u>S</u>ize on Chromosome <u>10</u>), which encodes a protein with 6 tandem armadillo repeats. The null mutant *gs10* shows slender and narrow grains with altered cell size, which has a pleiotropic effect on other agronomical traits. Functional analysis reveals that GS10 interacts with TUD1 (Taihu Dwarf1) and is epistatic to OsGSK2 (glycogen synthase kinase 2) through regulating grain shape and lamina joint inclination, indicating it is negatively involved in brassinosteroid (BR) signaling. Pyramiding *gs10* and the grain size gene *GW5* into cultivar GLA4 substantially improved grain shape and appearance quality. Natural variation analysis revealed that *gs10* from the wild rice *Oryza rufipogon* W1943 is a rare allele across the rice population. Collectively, these findings advance our understanding of the underlying mechanism of grain shape and provide the beneficial allele of *gs10* for future rice breeding and genetic improvement.

Introduction

Rice is one of the major cereal food crops in the world. Rice grain yield has been involved in many important agronomical traits, such as flowering time, plant height, grain size, and grain weight (Huang et al. 2016). Grain yield and grain quality are the 2 main determinants of modern rice breeding. The mechanisms underlying grain-size-related traits are mainly involved in the ubiquitin-proteasome pathway, G-protein signaling, mitogen-activated protein kinase signaling, phytohormone perception, and homoeostasis, and some transcriptional regulators (Li et al. 2019). More than 20

quantitative traits loci (QTLs) regarding grain size and quality have been characterized by QTL mapping and genome-wide association study (GWAS). The well-characterized G protein pathway determines grain size and grain weight in rice. Gα protein provides a foundation for grain size expansion, and Gβ is essential for plant survival and growth (Sun et al. 2018). Three Gγ proteins, DENSE AND ERECT PANICLE1 (DEP1), GGC2, and GS3, antagonistically regulate grain size. Furthermore, GS3 and DEP1 interact directly with OsMADS1 (qLGY3) to regulate grain size by enhancing OsMADS1 transcriptional activity and promoting the co-operative transactivation of common target genes (Liu et al. 2018; Yu et al. 2018). *GW2* encodes an unknown RING-type protein with E3 ubiquitin ligase activity involved in the ubiquitin-proteasome pathway, which regulates grain width (GW) and weight. Loss of *GW2* increases cell numbers, resulting in a larger (wider) spikelet hull and accelerating the grain milk filling rate (Song et al. 2007). Furthermore, *qSW5/GW5/GSE5* encodes a calmodulin-binding protein and physically interacts with OsGSK2, which is involved in brassinosteroid (BR) signaling for regulating GW and weight (Shomura et al. 2008; Weng et al. 2008; Duan et al. 2017; Liu et al. 2017). *GLW7* encoding the plant-specific transcription factor OsSPL13, identified by GWAS analysis on grain size in a diverse rice population, positively regulates cell size in the grain hull and enhances rice grain length and yield (Si et al. 2016). Although many related QTLs have been well characterized for grain size, the underlying molecular mechanisms of grain size regulation are still insufficiently addressed.

Grain quality (cooking, eating, and appearance quality) is closely associated with grain size in the hybrid rice population (Gong et al. 2017; Zhao et al. 2022). *GW8* encodes OsSPL16, which acts as a positive regulator for cell proliferation, GW, and grain filling in rice. The loss-of-function mutation *gw8* in the elite cultivar Basmati could cause more slender grain and better quality of appearance (Wang et al. 2012). *GL7/GW7* encoding a TONNEAU1-recruiting motif protein positively regulates grain length and improves rice yield and grain quality in rice (Wang et al. 2015a, 2015b). Besides, OsSPL16 (GW8) represses *GW7* expression by bounding directly to the *GW7* promoter. The OsSPL16-GW7 module provides a strategy to improve rice yield and quality in future rice breeding (Wang et al. 2015a). *GS9* encodes a protein with an unknown conserved functional domain and positively regulates grain shape by affecting cell division. *GS9* functions independently from other previously identified grain-size genes, and applying *gs9* null mutant substantially improves grain shape and appearance quality (Zhao et al. 2018a). Understanding the mechanism underlying gain size and quality can facilitate hybrid rice breeding with optimal grain shape and appearance quality.

Armadillo (ARM)-repeat proteins consist of a repeating ~42 amino acid motif that is conserved both in animals and in plants (Coates 2003). This superfamily has more than 100 ARM members in plants and animals, mainly involved in biotic, abiotic, and hormonal signaling networks (Tewari et al. 2010). In animals, the fascinating protein β-catenin (ARM in *Drosophila*) interacts with microtubules, which play an essential role in Wnt/β-catenin signaling to control multiple biological phenomena during the development and adult life of all animals (Tewari et al. 2010; Clevers and Nusse 2012). Unlike animals, the plant ARM subfamily where the ARM repeat region is preceded with a different motif, including F-box, U-box, and other domains, which may function diversely, such as cold stress response, stomatal movement, immune response, and other development processes (Zeng et al. 2004; Ngo et al. 2012; Hu et al. 2013; Sakamoto et al. 2013; Vogelmann et al. 2014; Jung et al. 2015). For example, 3 *Arabidopsis thaliana* ARMADILLO REPEAT ONLY (ARO) proteins interact with ROP1 enhancer GAPs (RENGAPs) and binding to the plasma membrane through the ARO amino terminus, which is essential for the stabilization of growth sites in root hair cells and trichomes (Kulich et al. 2020). The *spotted leaf11* (*spl11*) contains a U-box domain and 6 ARM repeats with E3 ubiquitin ligase activity, negatively regulating rice plant cell death and defense (Zeng et al. 2004). *Ptr* is reported as an atypical resistance gene with 4 ARM repeats, and targeted mutation of *Ptr* confers blast susceptibility in resistant cultivars (Zhao et al. 2018b). Even though ARM repeats play an essential role in many development processes, we know little about the mechanisms underlying grain shape and yield, especially in rice.

In our study, we characterized a gene, *GS10*, with 6 ARM repeats from wild rice. We demonstrated that *GS10* positively regulates grain size (especially grain length/GW) and that the allele *gs10* from wild rice could improve grain appearance quality without reducing total grain yield. Interestingly, pyramiding *gs10* with major beneficial grain size and quality gene *GW5* in the *Oryza sativa indica* cultivar GLA4 background results in increased grain length-to-width ratio and improved appearance quality, implying that loss-of-function allele *gs10* has the potentiality for grain quality improvement. We demonstrate that the tradeoff between grain size and grain quality in *GS10* facilitates our understanding of the mechanism of grain shape. This study also provides a new genetic framework and wild rice resources for improving rice breeding.

Results

Map-based cloning of *GS10* and polymorphism analysis

We developed backcross inbred lines (BILs) between the *O. sativa indica* variety Guangluai 4 (GLA4) and the wild rice *O. rufipogon* W1943. We mapped several grain-size related QTLs using this population, including the well-characterized genes *GW5/qSW5/GSE5*, *GL7/GW7*, and *GL6* (Shomura et al. 2008; Weng et al. 2008; Wang et al. 2015a, 2015b, 2019; Duan et al. 2017; Liu et al. 2017; Supplemental Fig. S1A). In terms of GW, QTL analysis revealed there is a semidominant GW and grain length to GW ratio QTL on chromosome 10 (Supplemental Fig. S1B).

To clone this gene, we chose the chromosome segment substitutional line 50 (CSSL50) as the parental line, with substitution of 5-Mb fragment from W1943 on chromosome 10 in the GLA4 background (Fig. 1A; Supplemental Fig. S2A). Compared to its recipient GLA4, the grain length of CSSL50 was not changed, while the GW, 1,000-grain weight, and grain thickness decreased by 9%, 10%, and 4%, respectively (Fig. 1, B and E–I). The locus was initially mapped between marker loci OP10-6 and OP10-7 using 155 BC_2F_2 plants and then fine-mapped to a 10-kilobase (kb) genomic region between marker loci SNP10-6 and SNP10-3 using the BC_2F_4 population ($n = 5,250$; Fig. 1, C and D). There was only a candidate gene within this region, *LOC_Os10g37850*, hereafter referred to as *GS10* (Fig. 1D).

Based on *GS10* sequence analysis (IRGSP 1.0), 4 polymorphisms were identified in the coding region between GLA4 and W1943, of which 2 SNPs lead to nonsynonymous mutation, and a 5-bp deletion can cause a frameshift and truncation of the predicted protein (Fig. 2A; Supplemental Fig. S3). These results suggested that the 5-bp deletion from wild rice may be the causative mutation for the slender and narrow grain in CSSL50.

Confirmation of *GS10* by the transgenic test

To characterize the genetic effect of the candidate gene, *GS10*, we first constructed a nearly isogenic line (NIL) containing a 170-kb chromosomal region from W1943 under the background of GLA4 (Supplemental Fig. S2B). In contrast to GLA4, NIL-*gs10* displays a pleiotropic effect on many agronomical traits, including panicle length, secondary branches, plant height, flag leaf length, flag leaf width, and grain yield per plant. Notably, *gs10* slightly decreases yield per plant but has a similar actual yield per plot to GLA4 (Supplemental Fig. S4).

To confirm whether *GS10* is responsible for the change of grain size, 2 complementary transgenic lines, CP-1 ($pGLA4$::$gGS10^{GLA4}$) and CP-2 ($pW1943$::$gGS10^{GLA4}$), based on the background of NIL-*gs10* were constructed, expressing the *GS10* $gDNA^{GLA4}$ fused with a native promoter from GLA4 and W1943, respectively (Fig. 2B). At least 10 individual T_0 transgenic lines were obtained, and we examined their GW and grain length/GW (Supplemental Fig. S5). Then, we constructed the overexpressing lines (OX, Ubi::$GS10^{GLA4}$) and knock-out lines *GS10*-CR (where CR indicates CRISPR-Cas9-induced) based on the GLA4 background (Fig. 2, B and C). There is no apparent difference in plant architecture except for plant height before grain filling. The plant height was increased by 7% in NIL-*gs10* and *GS10*-CR, while that of CP-1, *GS10*-OX, and CP-2 was decreased due to elevated gene expression (Supplemental Fig. S6). Besides, the results showed that CP-1 and CP-2 could rescue the phenotype in grain shape (grain length and GW) with a round and shorter grain compared with the NIL-*gs10* (Fig. 2, D and F–G). The *GS10*-OX exhibited a weaker difference in grain length and GW, but the *GS10*-CR showed a longer and narrower grain (Fig. 2, D and F–G). Regarding other agronomical traits, CP-1 and CP-2 decreased the panicle length and had no difference in grain weight and spikelets per panicle. The flag leaf length was longer in NIL-*gs10* and *GS10*-CR than in *GS10*-OX (Supplemental Fig. S7, B and C). The panicle length and spikelets per panicle were increased in NIL-*gs10* and *GS10*-CR, while the grain weight was decreased, suggesting *GS10* had a tradeoff between grain size, panicle number, and grain weight (Fig. 2, E and H–I; Supplemental Fig. S7D).

We also construct the transgenic lines using CRISPR-Cas9 in *japonica* lines. The grains formed by the 2 knock-out lines from Nipponbare (Nip) and Dongjin (DJ) significantly changed plant architecture, panicle length, and grain shape compared with its wild type (Supplemental Fig. S8). Consistently, we got a transfer DNA (T-DNA) insertion line (PFG_1C-02357.L) based on the *japonica* background "Hwayoung" (HY), named *gs10* (Supplemental Fig. S9, A and B). The T-DNA insertion site locates on the 1,480 bp upstream of the *GS10* coding region, and the expression of *GS10* was downregulated (Supplemental Fig. S9, C, D, and G). The complementary line HY-CP-1 showed wider and shorter grain than *gs10* (Supplemental Fig. S9, E and F). Taken together, these results demonstrated that *GS10* is the causative gene for the change of grain size.

Phylogenetic analysis revealed that *GS10* belongs to the ARM family, and amino acid sequence analysis showed that *LOC_Os03g02580* (*GS10-LIKE-PROTEIN 1*, *GSL1*) shared high sequence similarity with *GS10* (Fig. 2J; Supplemental Fig. 10A). To further investigate the genetic relationship between *GS10* and its homolog gene in rice, we designed 2 targets using CRISPR-Cas9 (Fig. 2K; Supplemental Fig. S11). As expected, *GSL1* also played an essential role in regulating grain size (e.g. GW and grain length/GW) like *GS10* but had a redundant function in the ARM subfamily (Fig. 2, M–N).

Expression pattern and subcellular localization of *GS10*

To investigate the expression pattern of *GS10*, we examine the transcript levels in various tissues in GLA4, including young panicles, flag leaf, leaf sheath, tiller bud, and endosperm. Reverse transcription quantitative PCR (RT-qPCR) revealed that the *GS10* transcript level was high in both younger seedlings and young panicles (Fig. 3A). These results suggested *GS10* might play an important role in leaf and panicle development. Observations during grain filling showed that the caryopsis of NIL-*gs10* was more slender than that of GLA4 from 7 days after fertilization (DAF) (Fig. 3, B and C).

To determine the subcellular localization of *GS10*, $p35S$::*GS10*-GFP (the full-length cDNA of GS10 fused to the N terminus of GFP) and NLS (nuclear localization signal)-RFP plasmids were transformed into rice, Arabidopsis protoplast or *Nicotiana benthamiana* epidermal cells, and the results showed GS10 localized in the cytoplasm (Fig. 3, D and E; Supplemental Fig. S12A). We also detected the subcellular localization between GW5 (plasma membrane marker) and GS10; the results showed GS10 mainly distributed in the cytoplasm (Supplemental Fig. S12B). The loss-of-function allele protein gs10 fused with GFP was also constructed and

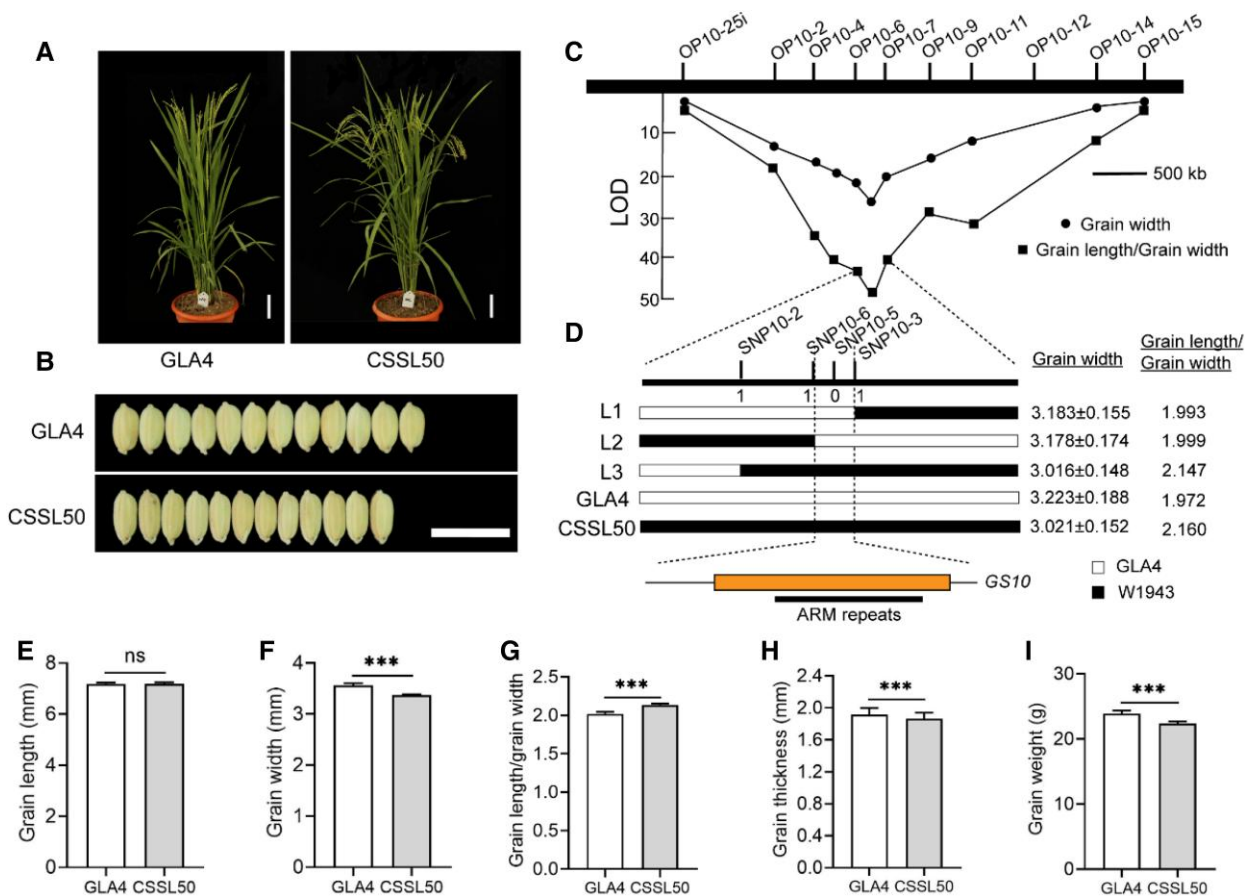**Figure 1.** Map-based cloning of *GS10*. Plant morphology and grain shape phenotype between GLA4 and CSSL50. Scale bar, 5 cm (**A**), 1 cm (**B**, both panels). **C)** *GS10* was initially mapped between marker loci OP10-6 and OP10-7 using 155 BC₂F₂ plants based on the phenotype of GW and grain length/GW. **D)** *GS10* was then fine-mapped to a 10-kilobase (kb) genomic region between the marker SNP10-6 and SNP10-3 using the BC₂F₄ population. Genotype (left), GW (middle), and grain length/GW (right) were shown for recombinant plants and the control plants. White and black bars represent chromosomal segments homozygous for GLA4 and W1943 alleles, respectively. The only 1 predicted open reading frame in the 10-kb delimited region among 3 CSSLs and their parents. The numbers below the molecular markers in (**D**) indicate the number of recombinants. Statistics of grain length **E)**, GW **F)**, grain length/GW **G)**, grain thickness **H)**, and grain weight **I)** between GLA4 and CSSSL50, $n \geq 18$. Values are given as the mean ± SD. Student's *t*-test significant difference, ***$P < 0.001$; ns, not significant.

transformed into *N. benthamiana* epidermal cells; the results showed that the truncated protein was distributed randomly in the cell and could not be appropriately located in the cytoplasm (Supplemental Fig. S12C).

GS10 regulates grain size by affecting cell size

The spikelet hull just before fertilization was much more slender in NIL-*gs10* than in GLA4 and the outer hull size depends upon the developmental processes of cell division and cell expansion (Fig. 4, A–C). Scanning electron microscopy observation showed no difference in cell number in the longitude and latitude of the outer surface of the glumes. The reduced cell width suggested that *GS10* might regulate grain size by affecting cell size (Fig. 4, C–E).

Meanwhile, we compared the expression level of cell division- and cell expansion-related genes in the young panicles of GLA4 and NIL-*gs10* using RT-qPCR. Only a small amount of cell division-related genes, like *CDKA2*, *CYCA2-3*,

CYCD4, *H1*, and *MCM3*, were significantly changed (Fig. 4F). But in terms of expansion genes, the expression of *OsEXPB3*, *OsEXPB4*, *OsEXPB5*, and *OsEXPB10* were increased in NIL-*gs10* (Fig. 4G). Taken together, we demonstrated that *GS10* regulated grain shape mainly by affecting cell expansion.

GS10 interacts with TUD1 that is involved in BR signaling

ARM repeat proteins play a vital role in regulating many biological processes in plants and animals (Tewari et al. 2010; Ye et al. 2012; Supplemental Fig. 10B). *GS10* encodes an unknown protein with only 6 ARM repeats, with many putative orthologs in land plants. *TUD1/ELF1* encodes a functional U-box E3 ubiquitin ligase and ARM repeats that interacts with *D1* (*RGA1*), which acts as a positive regulator of BR signaling by affecting plant height and grain size (Hu et al. 2013). TUD1 predominantly localizes to the plasma membrane and physically interacts with D1 (RGA1). We also investigated the relationship between
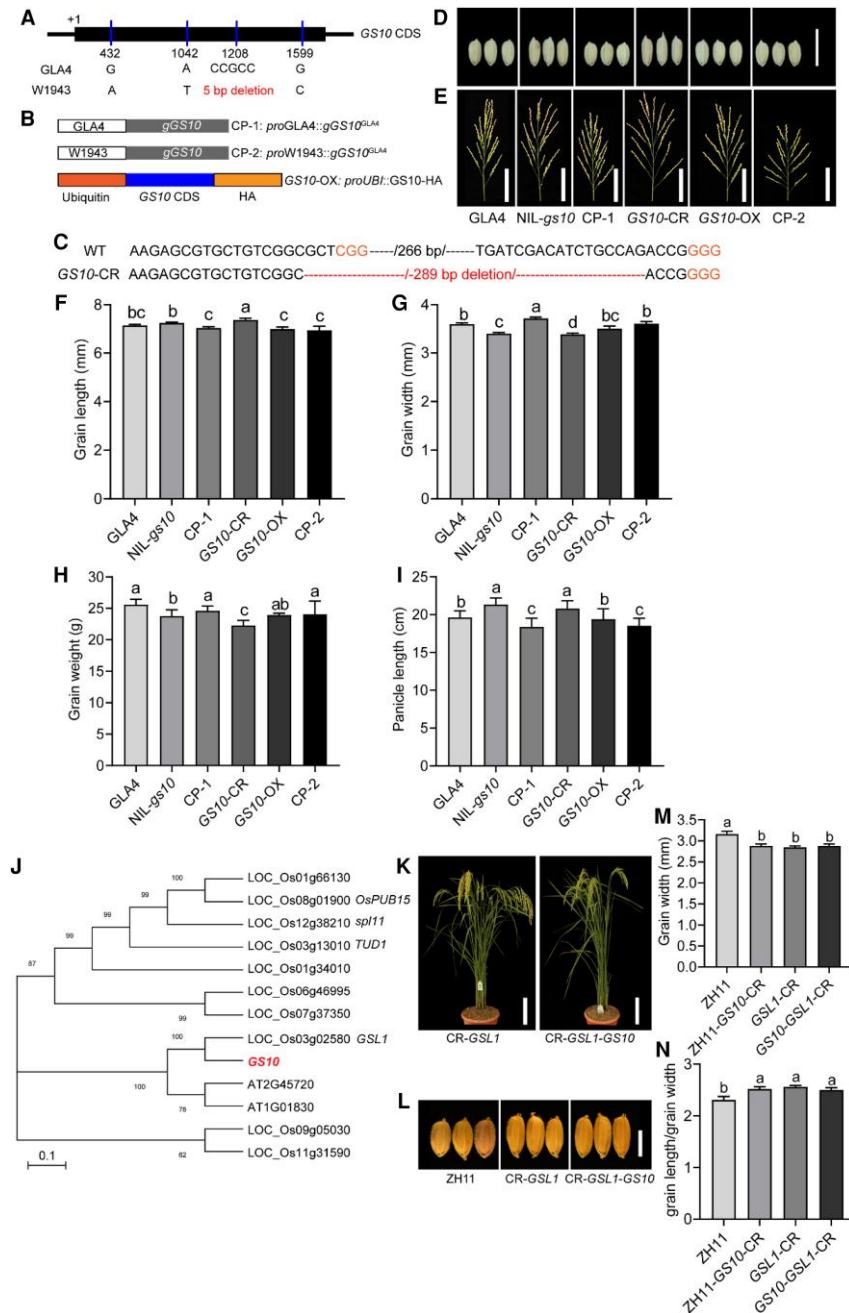
Figure 2. Conformation of *GS10* by the transgenic test. **A)** Schematic representation of gene structure and allelic variation of the *GS10*, the numbers below the gene bar indicate the number of polymorphic nucleotide(s) located in the coding region. The nucleotides of the causative mutation are in red. CDS, coding region sequence. **B)** Transgenic validation of GS10. Two complementary transgenic lines, CP-1 (*pGLA4::gGS10^GLA4*) and CP-2 (*pW1943::gGS10^GLA4*) were constructed, expressing the *GS10* gDNA^GLA4 fused with a native promoter from GLA4 and W1943 based on the background of NIL-*gs10*; the overexpressing lines (OX, *Ubi::GS10^GLA4*) and knock-out lines *GS10*-CR based on the GLA4 background. **C)** Schematic representation of CRISPR/Cas9-edited sequence in *GS10*-CR alleles. The *GS10*-CR mutant has a 289-bp deletion (the resulting knock-out region is in red) in the coding region. Confirmation by using the near-isogenic line. Morphology of grain shape **D)**, panicle **E)** of GLA4, the near-isogenic line NIL-*gs10*, and different transgenic lines (CP-1, *GS10*-CR, *GS10*-OX, and CP-2) during maturation from the field. Scale bars, 1 cm (**D**, for all panels), 5 cm (**E**). Comparison of grain length **F)**, GW **G)**, grain weight **H)**, and panicle length **I)** between different lines (GLA4, NIL-*gs10*, CP-1, *GS10*-CR, *GS10*-OX, and CP-2), $n = 6$. **J)** Phylogenetic analysis of putative ARM proteins in representative species. *OsPUB15*, *spl11*, and *TUD1* are all characterized genes. Scale bar, 0.1. **K)** Plant morphology phenotype between CR-*GSL1* and CR-*GS10-GSL1*. Scale bars, 10 cm. **L)** Grain shape between ZH11, CR-*GSL1*, and CR-*GS10-GSL1*. Scale bar, 5 mm (for all panels). **M, N)** Statistics of GW and grain length/GW between ZH11, CR-*GS10*, CR-*GSL1*, and CR-*GS10-GSL1*, $n = 6$. Values are given as the mean ± sd. As determined by Duncan's multiple-range test, lowercase letters indicate significant differences ($P < 0.05$).
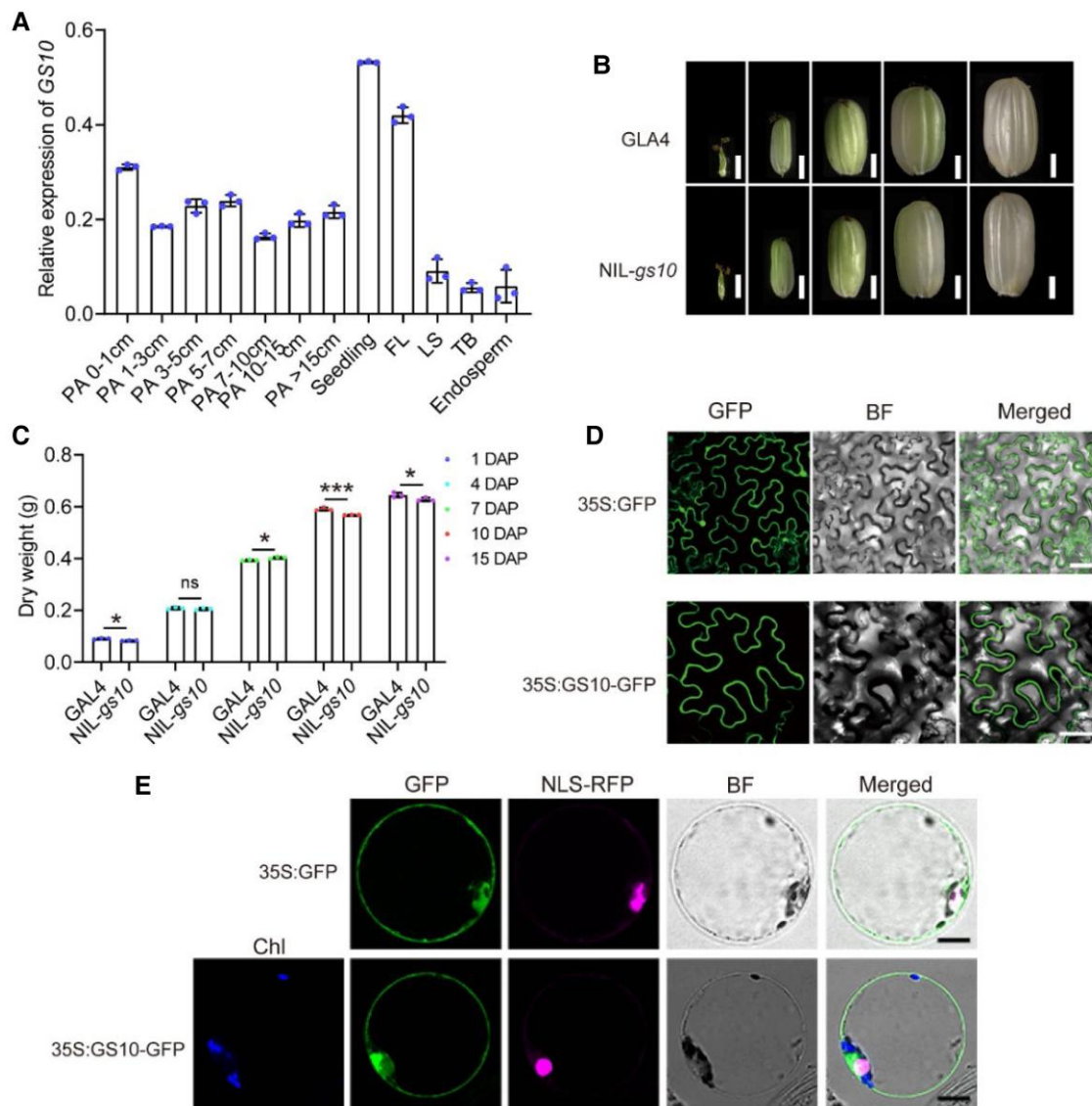
Figure 3. Expression pattern and subcellular localization of *GS10*. **A)** Relative expression of *GS10* in different tissues of GLA4. PA, panicle before heading; FL, flag leaf; LS, leaf sheath; TB, tiller bud. *OsUBQ5* was used as the control. Data are presented as mean values ± SD, $n = 3$ biologically independent samples. **B)** Comparison of the shape of developing caryopsis at indicated DAF between GLA4 (left) and NIL-*gs10* (right). Scale bars, 1 mm. **C)** Statistics of developing caryopsis dry weight at indicated days between GLA4 and NIL-*gs10*. Data are presented as mean values ± SD, $n = 3$ biologically independent samples. Subcellular localization of GS10 (35S::GS10-GFP) in *N. benthamiana* leaf **D)** and rice protoplasts **E)**. The plasmid 35S::GFP and NLS-RFP (nuclei marker) were used as the control. Scale bar, 10 μm **D)** and 20 μm **E)** in *N. benthamiana* leaf; 10 μm in rice protoplasts. Chl, chlorophyll. BF, bright field. Student's *t*-test significant difference, *$P < 0.05$ and ***$P < 0.001$; ns, not significant.

TUD1, D1, and GS10 using yeast-two-hybrid (Y2H), firefly luciferase (LUC) complementation imaging (LCI), and biomolecular fluorescence complementation (BiFC) assays (Fig. 5, A–C). Interestingly, GS10 could physically interact with TUD1 but not with D1, indicating GS10 may act as a membrane-interacting protein and be involved in BR signaling.

It is generally accepted that BR plays a vital role in many important agronomical traits of rice, including plant height, grain size, and lamina joint inclination (Tong and Chu 2018). From the transgenic test, we found that the CRISPR transgenic plants exhibited very loose plant architecture in both *indica* (*GS10*-CR) and *japonica* subspecies (DJ-CR and NIP-CR),

compared to its wild type (Fig. 5D; Supplemental Fig. S7A). Given that GS10 acts as a negative regulator in BR signaling, we tried to find the coregulator (mainly distributed in the cytoplasm) in the BR pathway. We firstly examined the relationship between GS10 and BR signaling-related genes, including *GW5-C2*, *OsBZR1*, *OsBRI1*, *OsBAK1*, *OsGSK2*, *OsGSK3*, and *OsGSK5*. Using Y2H, the results showed that GS10 could not interact with them (Supplemental Fig. S13A). Interestingly, we found OsOFP8 (OVATE Family Protein 8) could physically interact with GS10 (Supplemental Fig. S14, A–C; Yang et al. 2016). Previous studies have shown OsGSK2 can interact with OsOFP8 and phosphorylate it, and the phosphorylated
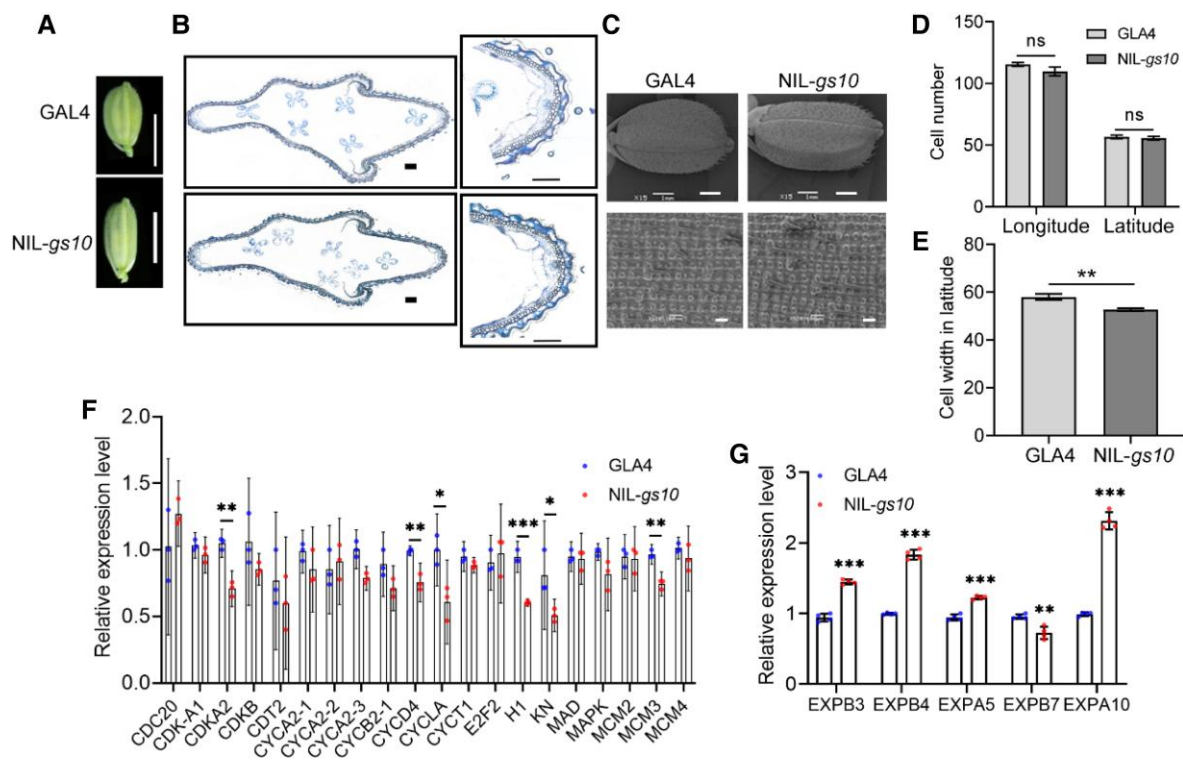
Figure 4. *GS10* regulates grain shape by altering cell size. **A)** Histological comparison of spikelet hulls between GLA4 and NIL-*gs10*. Scale bars, 5 mm. **B)** Cross-sections of spikelet hulls. The right images show closeup views of the boxed region. Scale bars, 100 μm. **C)** Scanning electron microscopy observation of the outer glumes between GLA4 and NIL-*gs10*. **D)** Cell number in longitude and latitude of glumes ($n = 4$). **E)** Statistics of cell width in latitude ($n = 4$). Relative expression levels of cell cycle-related genes **F)** and cell-expansion genes **G)** in young panicles (1 to 3 cm) of GLA4 and NIL-*gs10*. *OsUBQ5* was used as the control, and the expression levels in GLA4 were set to 1. $n = 3$ biologically independent samples. Values are given as the mean $\pm$ SD. Student's *t*-test significant difference: *$P < 0.05$, **$P < 0.01$ and ***$P < 0.001$; ns, not significant.

OsOFP8 could shuttle to the cytoplasm (Yang et al. 2016). Based on that study, we wondered whether GS10 could also affect the subcellular distribution of OsOFP8. Indeed, OsOFP8 shuttles to the cytoplasm in the presence of GS10, suggesting GS10 interacts with OsOFP8 by affecting its subcellular location (Supplemental Fig. S14D).

Considering the *OsGSK2*-OX line could dramatically affect plant height and grain size in rice, which is consistent with the transgenic lines *tud1* and *d1* (Liu et al. 2022). We also investigated the relationship between OsGSK2 and TUD1 using Y2H and LCI. The results showed that OsGSK2 could interact with TUD1, which is consistent with the previous studies (Supplemental Fig. S13, B and C; Liu et al. 2022). Furthermore, the double mutants *tud1-CR1*; *gs10-CR4* exhibited similar grain shape and plant height phenotype compared to the *tud1-CR1* (Supplemental Fig. S13, D–J). Besides, we constructed the double mutant lines (*OsGSK2-GS10-CR*) to investigate the genetic relationship between *OsGSK2* and *GS10*. Compared to *OsGSK2-CR* and *GS10-CR*-ZH11, the double mutant *OsGSK2-GS10-CR* showed a phenotype of loose plant architecture and larger leaf inclination (Fig. 5E; Supplemental Fig. S15, A and C). In terms of grain shape, the double mutant *GS10-OsGSK2-CR* showed a similar phenotype, indicating *GS10* was epigenetic to

OsGSK2 and may play a downstream role in BR signaling (Supplemental Fig. S15, B and D–H). We speculated that *GS10* might be involved in BR signaling by regulating grain size and leaf inclination, then we examined the relative expression of BR synthesis genes, including *D2*, *D11*, *OsBRD1*, *D61*, and *BU1*. Among them, the expression of *D2*, *D11*, and *OsBRD1* in NIL-*gs10* was increased compared to GLA4, indicating GS10 could negatively regulate BR synthesis (Supplemental Fig. S16). When treated with BL, the *GS10*-CR-ZH11 plant showed much longer coleoptile and larger leaf inclination than wildtype (Fig. 5, F–H).

Combining *GW5* and *GS10* can improve the appearance quality

GW5 and *GW7/GL7* are the 2 master genes identified in the BILs, regulating grain shape and grain quality, as previously reported (Shomura et al. 2008; Weng et al. 2008; Wang et al. 2015a, 2015b; Liu et al. 2017). To investigate the relationship between *gs10* and other grain size-related genes in future rice breeding, we got different pyramiding lines through the combination of NIL-*gs10*, NIL-*GW5*, and NIL-*GL7* (Fig. 6A). From the analysis of grain shape between NIL-*GW5/gs10*, NIL-*GL7/gs10*, and NIL-*gs10*, we found that

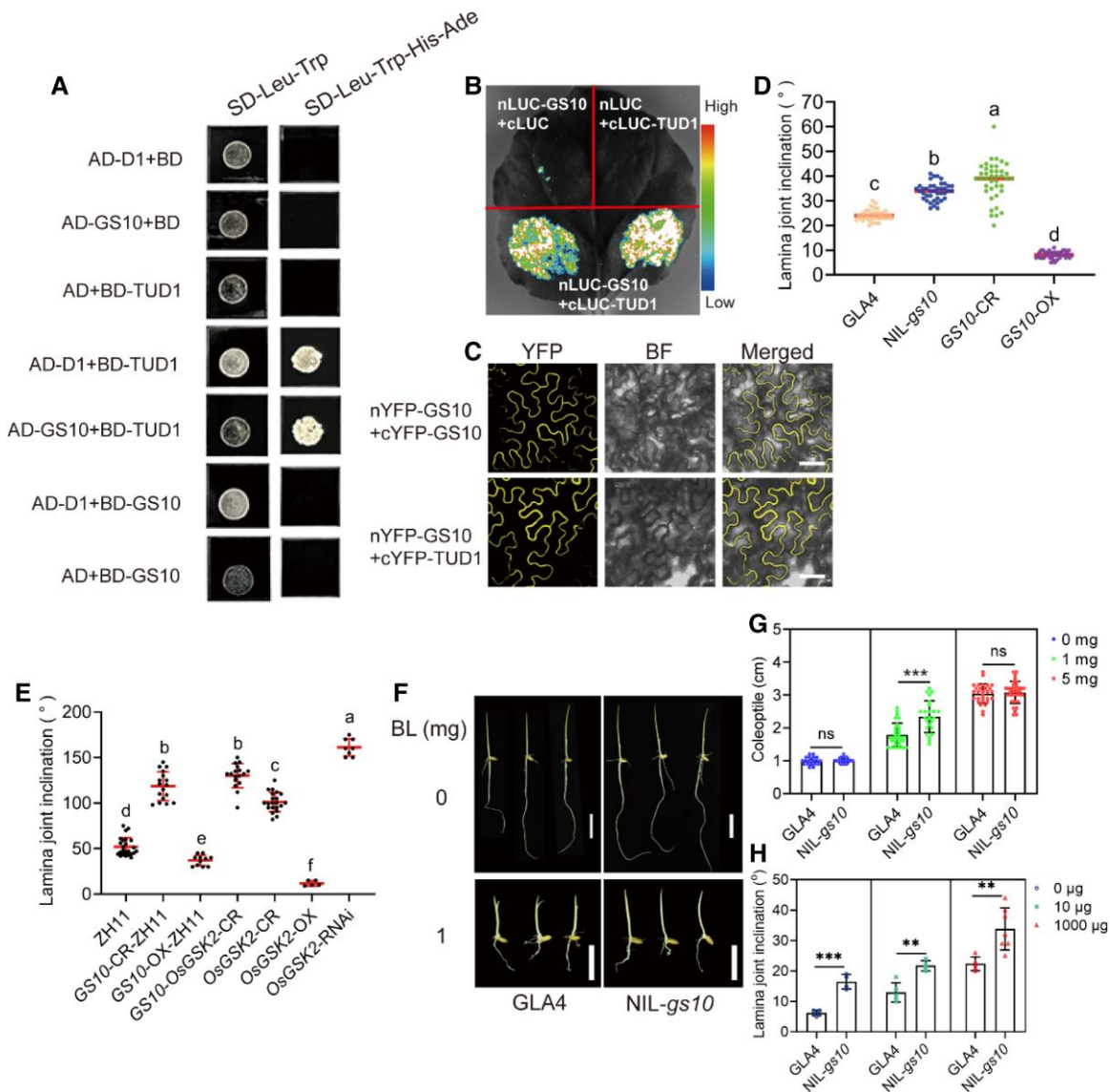**Figure 5.** GS10 interacts with TUD1, which is involved in BR signaling. **A)** Y2H assay of GS10, TUD1, and D1. AD, activation domain; BD, binding domain. SD–Leu–Trp–His–Ade (or SD–Leu–Trp), SD medium lacks Leu, Trp, Ade, and His (or lacks Leu, Trp). **B)** In vivo protein interaction of GS10 and TUD1 based on LCI in *N. benthamiana* leaf. **C)** BiFC assay between GS10 and TUD1 in *N. benthamiana* leaf. nYFP-GS10 and cYFP-GS10 were used as the control. BF, bright field. **D)** Statistics of lamina joint inclination in GLA4, NIL-*gs10*, *GS10*-CR, and *GS10*-OX. $n = 40$. **E)** Statistics of lamina joint inclination in ZH11, *GS10*-CR-ZH11, *GS10*-OX-ZH11, *GS10*-*OsGSK2*-CR, *OsGSK2*-CR, *OsGSK2*-OX, and *OsGSK2*-RNAi transgenic lines. $n \geq 40$. **F)** Comparison of 3-d seedlings after 0 and 1 mg BL treatment based on GLA4 and NIL-*gs10* background. BL, brassinolide. Scale bars, 1 cm. **G)** Statistics of coleoptile after 0 and 1 mg BL treatment based on GLA4 and NIL-*gs10* background. $n = 19$. **H)** Lamina joint inclination comparison of GLA4 and NIL-*gs10* after 0 and 1 mg BL treatment, $n \geq 4$. As determined by Duncan's multiple-range test, lowercase letters indicate significant differences ($P < 0.05$). Values are given as the mean ± SD. Student's *t*-test significant difference: *$P < 0.05$, **$P < 0.01$, and ***$P < 0.001$; ns, not significant.

gs10 has an additive effect on *GW7* and *GW5* in both GW and grain length/GW, while the grain weight was decreased in pyramiding line NIL-*gs10/GL7*, NIL-*gs10/GW5*, indicating *GS10* regulate grain size independent of *GL7/GW7* and *GW5*. Consequently, the grain weight of *GW5/GW7/gs10* was significantly changed, which was reduced by 20%, suggesting that introgressing *gs10* into cultivars could improve grain shape and appearance quality but reduce grain yield (Fig. 6, B–D).

To date, grain shape change (especially the grain length/GW ratio) is closely associated to grain quality (Wang et al. 2012; Liu et al. 2018). For transparency of the brown rice, NIL-*gs10* shows no obvious change in chalkiness compared to GLA4 in terms of the percentage of chalky grain and chalkiness degree (Fig. 7). Interestingly, pyramiding *gs10* and *GW5* into GLA4 can significantly produce much better quality, as well as improve grain shape and reduce chalkiness (Supplemental Fig. S17A). To further investigate the inner grain quality of *gs10*, we detected
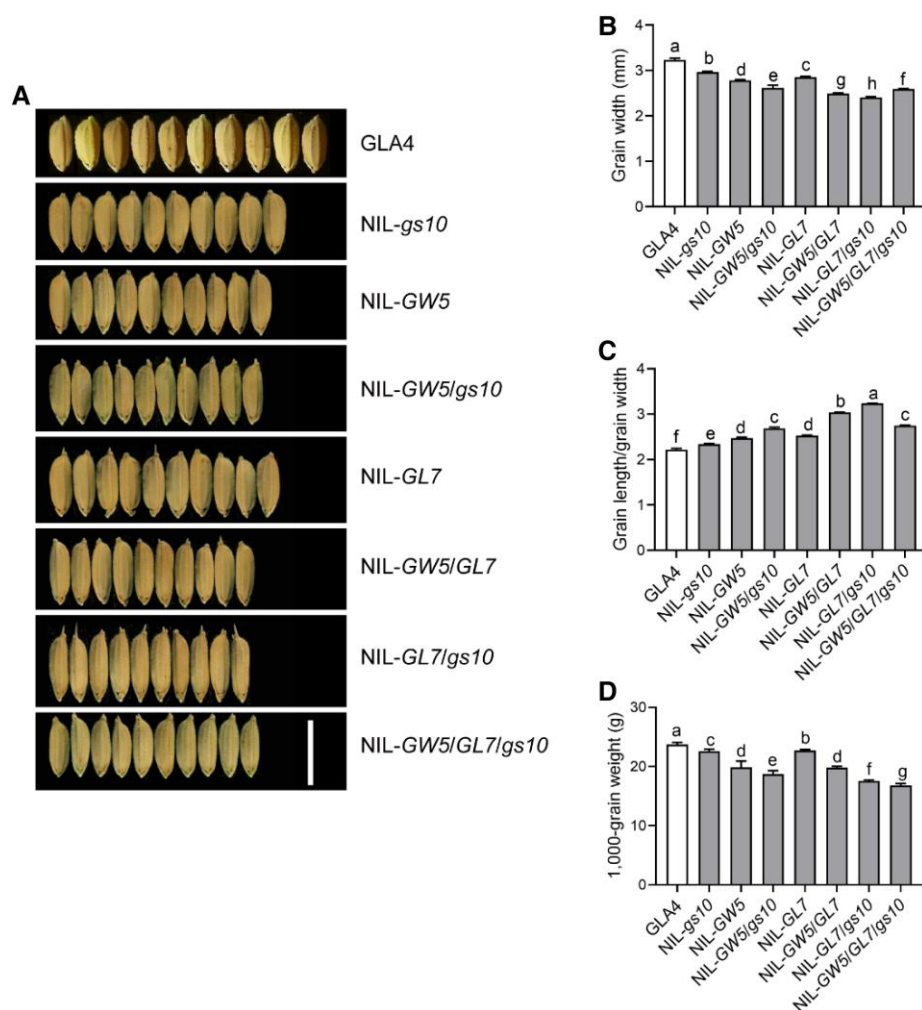
Figure 6. Relationship between gs10 and other grain-size QTLs. **A)** Phenotypes of grain shape between different pyramiding lines. The pyramiding lines NIL-*gs10/GL7*, NIL-*gs10/GW5*, NIL-*GL7/GW5*, and NIL-*gs10/GW5/GL7* were constructed through the combination between NIL-*gs10*, NIL-*GW5*, and NIL-*GL7* (also referred to NIL-*GW7*); NIL-*GW5*, the near-isogenic line contains the *GW5* allele in GLA4; NIL-*GL7/GW7*, the near-isogenic line has the *GL7/GW7* allele in GLA4; Scale bar, 1 cm (for all panels). Comparison of GW **B)**, grain length/GW **C)** and 1,000-grain weight **D)** between different pyramiding lines, *n* = 6. Values are given as the mean ± SD. As determined by Duncan's multiple-range test, lowercase letters indicate significant differences (*P* < 0.05).

taste value, protein content, apparent amylose content, and fatty acid content using the taste analyzer. Intriguingly, we found that *gs10* could slightly decrease protein content but not affect taste value, obvious amylose content, and fatty acid content (Supplemental Fig. S17, B–E). Besides, *GW5* and *gs10* significantly improve the taste value by decreasing protein content and apparent amylose content compared to *GW5* and *GS10*.

Natural variation of *GS10*

To further uncover the natural variation in the rice population, 111 wild rice accessions and 989 landraces (including 19 aus, 5 aromatic, 22 intermedia, 539 indica, 49 tropical japonica, and 363 temperate japonica) were selected to investigate the natural variation of *GS10* (Huang et al. 2012). Based on the sequencing of the coding region of *GS10*, 11 polymorphic sites, including 7 SNP and 5 insertions or deletions (InDels), were

identified to form 16 haplotypes across the whole rice species (Supplemental Fig. S18, A, B and Data Set S1). The wild rice population was classified into 13 haplotypes, of which 6 with insertion–deletion mutation may cause a premature stop in the coding region. But in landraces, the population could be divided into 6 haplotypes, of which the allele that causes loss-of-function mainly within *aus* and *aromatic*.

Previous studies have assumed that a selective sweep conferring GW exists within the flanking region of *GS10* (Huang et al. 2012). We also tested whether *GS10* is a domesticated gene that regulates grain size during domestication using Tajima's *D* test, indicating *GS10* is not a domestication gene (Fig. 8A; Supplemental Fig. S18C). Comparative analysis revealed that *gs10* from W1943 is a rare allele across the rice population. Allelic mutation of *GS10* in the wild rice population may act as a natural pool to provide more variations to improve rice appearance quality.
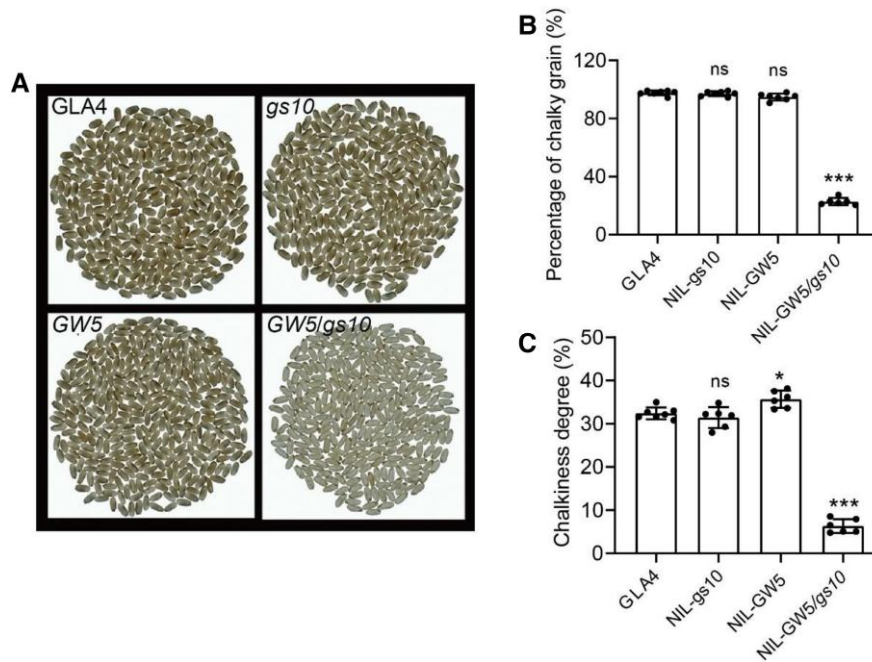
Figure 7. Pyramiding *gs10* and *GW5* could significantly improve rice grain appearance quality. **A)** The shape of milled rice of NIL-*gs10*, NIL-*GW5*, and NIL-*GW5/gs10* and its recipient GLA4. Decreased chalkiness in milled rice of NIL-*GW5/gs10* compared with those of GLA4. Statistics of the percentage of chalky grain **B)** and chalkiness degree **C)** between GLA4, NIL-*gs10*, NIL-*GW5*, and NIL-*GW5/gs10*; n = 6. Values are given as the mean ± SD. Student's *t*-test significant difference: *P < 0.05 and ***P < 0.001; ns, not significant.

Discussion

GS10 confers grain size and grain quality

The Tandem repeated protein family, which widely exists in plants and animals, plays a vital role in the growth and development process (Coates 2003; Barkan and Small 2014). There are 158 ARM proteins in rice (Sharma et al. 2014). However, limited mechanisms of this superfamily have been characterized to date. Research on plant ARM proteins has mainly focused on plant U-box (PUB) subfamily proteins. The PUB proteins contain a modified RING domain (U-box E3 ligases), which is known to be involved in biotic stress responses through the ubiquitin-proteasome system. Nevertheless, the subfamily proteins with 6 ARO proteins are mostly unknown.

In our study, we cloned a gene *GS10* with 6 ARO from wild rice, a component that regulates grain size by affecting cell size (Fig. 8B). We proposed that *GS10* has a pleiotropic effect on many agronomic traits, which might coincide with its transcriptome regulation. Notably, the allele *gs10* from W1943 displays the slender and narrow grain, improving appearance quality without reducing grain yield and overcoming the trade-off between grain quality and yield (Supplemental Fig. S4).

GS10 acts as a negative regulator involved in BR signaling

BRs play a vital role in plant growth and development (Tong and Chu 2018). OsGSK2, homologs of AtBIN2 and GSK3, acts as a central kinase in BR signaling in Arabidopsis and rice

(Tong and Chu 2018). OsGSK2 interacts with and phosphorylates many BR downstream proteins, like OsOFP8, OsGRF4/GL2, and OsBZR1 (Che et al. 2016; Yang et al. 2016; Fang et al. 2020). Unlike plants, GSK3 interacts with and phosphorylates β-catenin or Arm coupling with Axin and APC (Youn and Kim 2015). From our results, TUD1 could interact with GS10, but GS10 could not physically interact with OsGSK2 and D1, indicating GS10 might act as a plasma membrane interacting protein, participating in the G protein module (D1-TUD1-GS10) and BR signaling (OsGSK2-OsOFP8-GS10) (Fig. 5). We speculated that GS10 regulated grain shape and plant architecture in an OsGSK2-OsOFP8-dependent manner. For the potential mechanism of the TUD1-GS10 module involved in BR signaling, TUD1 might modulate the stability of GS10 in a ubiquitin-dependent manner. This hypothesis requires further research.

In our study, we demonstrate GS10 interacts with TUD1 which is involved in BR signaling, then regulating grain shape and plant architecture. We tried to address the protein relationship between GS10, TUD1, and OsGSK2. Recently, a paper demonstrated that TUD1 promotes BR-induced OsGSK2 degradation in rice (Liu et al. 2022). In their model, TUD1 could interact with OsGSK2 which is involved in BR signaling. We found GSK2 could interact with TUD1 in SD−Leu−Trp−His, rather than in SD−Leu−Trp−His−Ade (Supplemental Fig. S13B). We also use LCI to validate it (Supplemental Fig. S13C). The double mutant *tud1-CR1*; *gs10-CR4* has similar grain shape and plant architecture phenotype compared to *tud1-CR1*, indicating *TUD1* is epistatic to *GS10* (Supplemental Fig. S13,
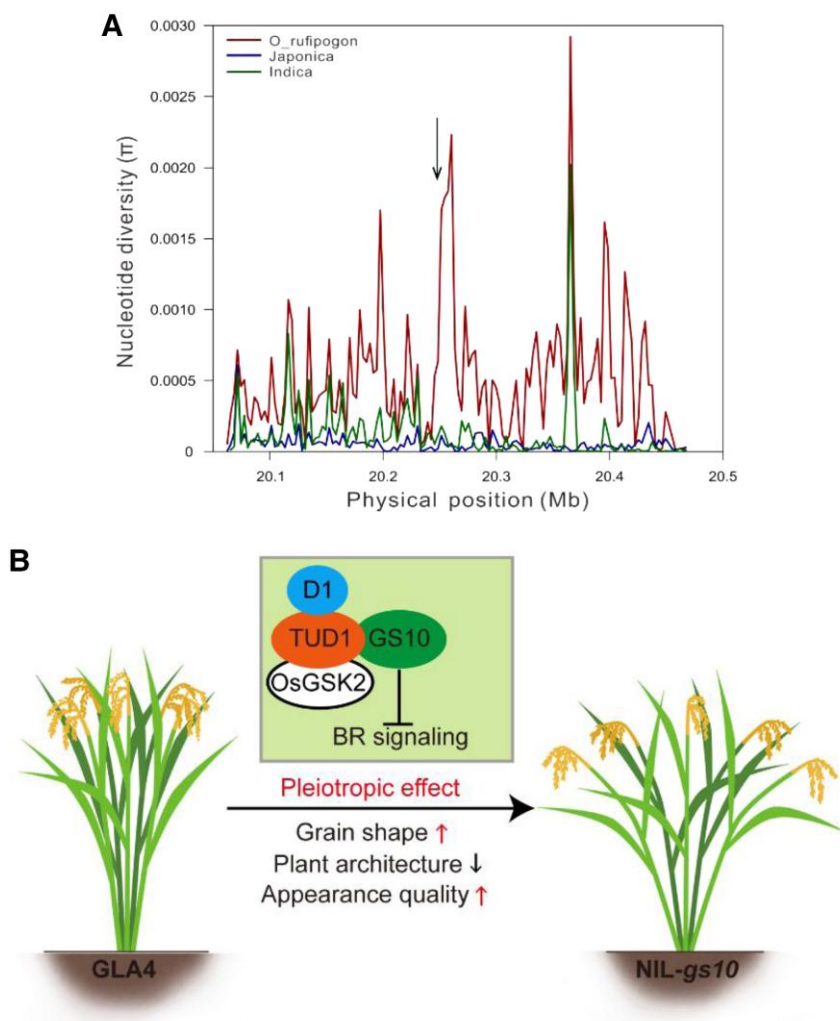
Figure 8. Natural variation of *GS10* in rice population. **A)** Genetic diversity around the *GS10* region. Red, green, and blue lines indicate nucleotide diversity (π) of all sites in *O. rufipogon*, *O. indica*, and *O. japonica*, respectively. The arrow indicates the position of *GS10*. **B)** A proposed working model of *GS10* for regulating grain shape, plant architecture, and grain quality.

D–I).The mutant *tud1-CR1* has striking phenotype that is involved in BR signaling, we want to uncover whether TUD1 promotes GS10 degradation at the protein level in the future. In our system, we assumed that TUD1 and OsGSK2 have a weak interaction at protein level. So, we assumed that GS10, TUD1, and OsGSK2 may form a protein complex in BR signaling. We want to investigate the relationship between GS10 and OsGSK2, and the results showed OsGSK2 could not interact with GS10. We construct the double mutants CR-*GS10-OsGSK2* to further demonstrate that GS10 is indeed involved in BR signaling.

We also found that *GS10-CR* transgenic plants in *indica* and *japonica* lines exhibited a BR-sensitive phenotype, indicating that *GS10* could affect BR syntheses- and signaling-related gene expressions, like *D2*, *D11*, and *OsBRD1* (Supplemental Fig. S17A). *GS9* encodes an unknown transcription activator interacting with OsOFP14 and OsOFP8 to regulate grain shape and quality (Zhao et al. 2018a). We also got the targeted

double mutant line *GS9-GS10-CR* using CRISPR-cas9, showing that *GS10* had an addictive effect on grain length and GW with *GS9*, resulting in a more slender and narrower grain hull (Supplemental Fig. S19). We assumed that *GS10* might function dependently on *GS9* in BR signaling, and the resulting *GS9-GS10-CR* mutant could further improve grain shape.

GS10 is a rare allele and has the potential for future breeding

The null mutant *gs10* with a slender and narrow grain could affect apparent amylose and protein contents to regulate grain quality. Pyramiding *gs10* and *GW5* could substantially improve the appearance quality of brown rice, and these results were consistent with the mechanism underlying grain quality of *GW8* and *OsMADS1* (Fig. 7; Supplemental Fig. S17; Wang et al. 2012; Liu et al. 2018). Previous studies have shown that GW5 acted as a domestication gene conferring GW and quality, favored in modern cultivars (Liu et al.

2017). We speculated that the rare allele *gs10* was not favored to be selected during domestication, which might be attributed to its negative role in pyramiding breeding regarding grain weight. We also analyzed the milled rice rate between GLA4 and NIL-*gs10*, and *GS10* could change the speed of milled rice by regulating cell size, thereby improving grain quality in rice (Fig. 3, B and C).

In summary, *GS10* could balance grain yield, plant architecture, and grain quality during rice domestication. In the future, the wild rice population should be used as a natural resource to identify more beneficial alleles of *GS10*, thus improving grain quality. We confirm that the *GW5-gs10* pyramiding lines will provide a strategy for improving the grain quality in hybrid rice.

Materials and methods

Plant materials, trait measurement, and BL treatment

All the rice materials grew in the experimental field in Shanghai and Hainan, China. The grain length, GW, and grain weight of mature seeds were measured by the image method provided with SC-E software (Hangzhou Wanshen Detection Technology Co., LTD). For inner grain quality, we measured taste value, protein content, apparent amylose content, and fatty acid content using the taste analyzer (SATAKE). The elite breeding line Koshihikari was used as the control, and the taste value is 78.

For the BL treatment assay, the lamina inclination assay was performed as previously described (Hong et al. 2003). Plants were grown for 3 d (d) after 2-d germination at 30 °C. Then, ethanol (1 mL) containing 0, 10, 100, or 1,000 ng of BL (sigma) was spotted on the top of the lamina. Images were taken after a 3-d incubation, and the angles of lamina joint inclination bending were measured.

Molecular mapping of *GS10*

For the fine-mapping of *GS10*, we developed 5,250 BC$_2$F$_4$ populations derived from the backcross between CSSL50 and the recipient parent GLA4. The mapping primers were designed based on the reference genome of GLA4 and W1943, and the primer sequences are given in Supplemental Data Set 2.

Histological analysis

For the cross-sections, fresh young spikelet hulls were fixed in formaldehyde:acetic acid (FAA: 50% [v/v] ethanol = 5:5:90), dehydrated, embedded in Eponate 12 (Ted Pella), and then sectioned. Cross-sections were captured by Zeiss Axio imager.M2, and the cell number in the outer parenchyma cell layer of hulls was measured using ImageJ.

Mature seeds were first cleaned ultrasonically several times to remove epidermal hairs and dust. The samples were then dried in a critical point drier and coated with a gold sputter. For glume cell observation, the outer surfaces of the spikelet glumes were observed by scanning electron microscope (S-4800, Hitachi). Cell size and cell number were calculated along the longitudinal axis. For starch granule observation, natural cross-sections of mature milled rice were observed by scanning electron microscope.

Vector construction and rice transformation

For the complementary test, we constructed the 2 kinds of complementary plasmids, CP-1, and CP-2. The 3-kb promoter fragments of GS10 were amplified from GLA4 and W1943 with the primers. The genomic sequence containing the GS10 promoter from GLA4 fused with the coding region of *GS10* from GLA4 was inserted into the pCAMBIA1300 binary vector to generate the CP-1 (*pGLA4::gGS10^{GLA4}*) expression vector. Similarly, CP-2 (*pW1943::gGS10^{GLA4}*) was generated using the promoter of GS10 from W1943 and the cDNA of GS10 from GLA4.

For overexpressing construction, the coding region of *GS10* was amplified and then introduced into pCAMBIA1300 under the control of the maize *ubiquitin* promoter. To knock out genes by CRISPR-Cas9, the sgRNAs of *GS10*, *GSL1*, *OsGSK2*, and *GS9* were selected by CRISPR-P 2.0 (http://crispr.hzau.edu.cn/CRISPR2/) (Ma et al. 2015). The above-constructed plasmids were then transformed into rice callus using *Agrobacterium tumefaciens*-mediated methods. Each T$_0$ transgenic plant with positive lines was more than 10 lines. The above primer sequences are given in Supplemental Data Set 2.

Y2H assays

The Y2H assay was performed according to the manufacturer's instructions (Clontech). The coding region of GS10, TUD1, GSL1, GW5-C2 (Liu et al. 2017), OsBZR1, OsBRI1, OsBAK1, OsGSK2, OsGSK3, OsGSK5, and OsOFP8 were amplified and then inserted into pGBKT7 or pGADT7. The constructed vectors were transformed into yeast strain AH109 or Y2H. The yeast cells were spotted on the plates that contain SD medium lacking Leu, Trp, Ade, and His. The pictures were taken 3 d later after incubation at 30 °C.

BiFC, LCI, and subcellular localization

For BiFC and LCI, the coding region of GS10, TUD1, GSL1, OsGSK2, and OsOFP8 were amplified and fused with the N terminal or C terminal of YFP and LUC, respectively. For subcellular localization, the CDS of *GS10*, *GW5*, and *OsOFP8* were inserted into 35S-GFP and 35S-mCherry. The NLS sequence was fused in-frame with RFP into PA7-35S-RFP as a nuclear marker. The constructed plasmids were transformed into *N. benthamiana* leaves or rice protoplasts. *Agrobacterium tumefaciens* GV3101, suspended in infiltration buffer (10 m$_M$ MgCl$_2$, 10 m$_M$ methyl ester sulfonate, 150 μ_M acetosyringone) and then expressed in the leaves of *N. benthamiana*. Fluorescence was observed by confocal microscopy (ZEISS880; Carl Zeiss). YFP signals were excited at 514 nm and emission was detected at 520 to 545 nm. For LCI assay, the sample leaves were injected with 1× luciferin, and the resulting LUC signals were detected using the Tanon-5200M image system.

RNA extraction and RT-qPCR

Total RNA was extracted using the TRIzol reagent (Invitrogen) according to the manufacturer's instructions. Then 500 to 1,000 ng of total RNA was used to synthesize the first-strand cDNA using ReverTra Ace qPCR RT Master Mix with gDNA Remover (Toyobo). RT-qPCR was performed on the Applied Bio-systems QuantStudio 5 PCR system with diluted cDNA as a template using THUNDERBIRD SYBR qPCR Master Mix (Toyobo), and *OsUBQ5* was used as a control. Each set of experiments was repeated 3 times.

Phylogenetic analysis

Homologs of GS10 in rice and *A. thaliana* were obtained using the NCBI BLASTP program (Supplemental Data Set 3). Multiple sequence alignments of protein were performed using the ClustalW program. The phylogenetic tree of the aligned sequence was constructed by MEGA-X using a neighbor-joining tree with 1,000 bootstrapped replicates. A graphic view was displayed as black color, indicating identical or conserved amino acids, respectively.

Haplotype analysis and neutrality test

For *GS10* nature variation analysis, the landraces were collected and sequenced in low coverage (Huang et al. 2012). The sequence of *GS10* was aligned using Blast (Version 2.2.26) to confirm the target sequence. Then target sequences in the rice population were extracted using a customized Perl script, and the diffseq program further called sequence variants in the EMBOSS package (Version 4.0). Haplotype analysis for *GS10* among the rice population was conducted by customized Perl script. Nucleotide diversity and Tajima's *D* test were performed using DnaSP version 6.12.03 (Rozas et al. 2017).

Statistical analysis

Statistical analyses were carried out using GraphPad Prism software (Version 8.0) and Microsoft Excel 2010 with a 2-tailed Student's *t*-test for the comparison of 2 groups and R package "agricolae" with Duncan's multiple-range tests for multiple mean comparisons.

Accession numbers

The sequence data from this article can be found on the China Rice Data Center website (http://www.ricedata.cn/gene/) under the following accession numbers: *GS10* (LOC_Os10g37850), *GSL1* (LOC_Os03g02580), *TUD1/ELF1* (LOC_Os03g13010), *OsOFP8* (LOC_Os01g64430), and *OsGSK2* (LOC_Os05g11730).

Acknowledgments

Author Contributions

B.H. conceived the research; E.C. and B.H. designed the study. E.C. performed most of the experiments. E.C., Q.H., K.L., B.D., J.Z., Y.S., D.L., and Z.W. all performed the experiments; Z.G. Y.Z. and X.H. did the informatics analysis; E.C., Q.H., K.L., A.W., Y.W., and Z.W. were responsible for field management and phenotype investigation; T.H. managed server station; Q.F., C.Z., and D.F. performed library construction and whole genome sequencing; E.C. and B.H. wrote the article; E.C., Q.H., K.L., and B.H. read and approved the writing.

Supplemental data

The following materials are available in the online version of this article.

Supplemental Figure S1. Identification and selection of grain size-related QTLs derived from the BILs of W1943 and GLA4.

Supplemental Figure S2. Identification and selection of the NIL-*gs10*.

Supplemental Figure S3. Comparison of nucleic acid and protein sequences between 2 different *GS10* alleles of GLA4 and W1943 (supports Fig. 2).

Supplemental Figure S4. Comparison of other important agronomic traits between GLA4 and NIL-*gs10*.

Supplemental Figure S5. Comparison of GW and grain length/GW between 2 T_1 complementary lines (CP1-T_1 and CP2-T_1).

Supplemental Figure S6. Analysis of plant architecture and relative expression levels in different lines (supports Fig. 2).

Supplemental Figure S7. The lamina inclination and flag leaf comparison between GLA4, NIL-*gs10*, GS10-CR, and GS10-OX (supports Fig. 2).

Supplemental Figure S8. *GS10* knock-out line in *japonica* backgrounds using CRISPR-Cas9.

Supplemental Figure S9. *GS10* transgenic validation using T-DNA mutant.

Supplemental Figure S10. Diagram of the ARM protein structure.

Supplemental Figure S11. Protein sequence comparison and *GSL1* gene-editing analysis using CRISPR-Cas9.

Supplemental Figure S12. Subcellular localization of GS10 (supports Fig. 3).

Supplemental Figure S13. Y2H assay analysis and protein interaction validation between TUD1 and OsGSK2 (supports Fig. 5).

Supplemental Figure S14. In vivo and in vitro analysis of the interaction between GS10 and OsOFP8.

Supplemental Figure S15. Genetic analysis of plant architecture and grain size between *GS10* and *OsGSK2* transgenic lines (supports Fig. 5).

Supplemental Figure S16. Relative expression of BR synthesis genes.

Supplemental Figure S17. Comparison of appearance and taste quality between GLA4, NIL-*gs10*, NIL-*GW5*, and NIL-*gs10*/*GW5* (supports Fig. 7).

Supplemental Figure S18. Haplotype analysis and Tajima's *D* test across the rice population (supports Fig. 8).

Supplemental Figure S19. Genetic analysis between *GS9* and *GS10* using CRISPR-Cas9.

Supplemental Data Set S1. The coding region sequencing of *GS10* across the rice population.

Supplemental Data Set S2. Primers were used in the study.

Supplemental Data Set S3. Phylogenetic analysis of putative ARM proteins in representative species.

Funding

Data availability

All data are available from the corresponding author upon requests.

References

Barkan A, Small I. Pentatricopeptide repeat proteins in plants. Annu Rev Plant Biol. 2014:**65**(1):415–442. https://doi.org/10.1146/annurev-arplant-050213-040159

Che R, Tong H, Shi B, Liu Y, Fang S, Liu D, Xiao Y, Hu B, Liu L, Wang H, et al. Control of grain size and rice yield by GL2-mediated brassinosteroid responses. Nat Plants. 2016:**2**(1): 15195. https://doi.org/10.1038/nplants.2015.195

Clevers H, Nusse R. Wnt/beta-catenin signaling and disease. Cell. 2012:**149**(6): 1192–1205. https://doi.org/10.1016/j.cell.2012.05.012

Coates JC. Armadillo repeat proteins: beyond the animal kingdom. Trends Cell Biol. 2003:**13**(9): 463–471. https://doi.org/10.1016/S0962-8924(03)00167-3

Duan P, Xu J, Zeng D, Zhang B, Geng M, Zhang G, Huang K, Huang L, Xu R, Ge S, et al. Natural variation in the promoter of GSE5 contributes to grain size diversity in rice. Mol Plant. 2017:**10**(5): 685–694. https://doi.org/10.1016/j.molp.2017.03.009

Fang Z, Ji Y, Hu J, Guo R, Sun S, Wang X. Strigolactones and brassinosteroids antagonistically regulate the stability of the D53-OsBZR1 complex to determine FC1 expression in rice tillering. Mol Plant. 2020:**13**(4): 586–597. https://doi.org/10.1016/j.molp.2019.12.005

Gong JY, Miao JS, Zhao Y, Zhao Q, Feng Q, Zhan QL, Cheng BY, Xia JH, Huang XH, Yang SH, et al. Dissecting the genetic basis of grain shape and chalkiness traits in hybrid rice using multiple collaborative populations. Mol Plant. 2017:**10**(10): 1353–1356. https://doi.org/10.1016/j.molp.2017.07.014

Hong Z, Ueguchi-Tanaka M, Umemura K, Uozu S, Fujioka S, Takatsuto S, Yoshida S, Ashikari M, Kitano H, Matsuoka M. A rice brassinosteroid-deficient mutant, ebisu dwarf (d2), is caused by a loss of function of a new member of cytochrome P450. Plant Cell. 2003:**15**(12):2900–2910. https://doi.org/10.1105/tpc.014712

Hu X, Qian Q, Xu T, Zhang Y, Dong G, Gao T, Xie Q, Xue Y. The U-box E3 ubiquitin ligase TUD1 functions with a heterotrimeric G alpha subunit to regulate brassinosteroid-mediated growth in rice. PLoS Genet. 2013:**9**(3): e1003391. https://doi.org/10.1371/journal.pgen.1003391

Huang XH, Kurata N, Wei X, Wang ZX, Wang A, Zhao Q, Zhao Y, Liu K, Lu H, Li W, et al. A map of rice genome variation reveals the origin of cultivated rice. Nature. 2012:**490**(7421): 497–501. https://doi.org/10.1038/nature11532

Huang XH, Yang SH, Gong JY, Zhao Q, Feng Q, Zhan QL, Zhao Y, Li WJ, Cheng BY, Xia JH, et al. Genomic architecture of heterosis for yield traits in rice. Nature. 2016:**537**(7622): 629–633. https://doi.org/10.1038/nature19760

Jung C, Zhao PZ, Seo JS, Mitsuda N, Deng SL, Chua NH. PLANT U-BOX PROTEIN10 regulates MYC2 stability in Arabidopsis. Plant Cell. 2015:**27**(7): 2016–2031. https://doi.org/10.1105/tpc.15.00385

Kulich I, Vogler F, Bleckmann A, Cyprys P, Lindemeier M, Fuchs I, Krassini L, Schubert T, Steinbrenner J, Beynon J, et al. ARMADILLO REPEAT ONLY proteins confine rho GTPase signaling to polar growth sites. Nat Plants. 2020:**6**(10): 1275–1288. https://doi.org/10.1038/s41477-020-00781-1

Li N, Xu R, Li Y. Molecular networks of seed size control in plants. Annu Rev Plant Biol. 2019:**70**(1): 435–463. https://doi.org/10.1146/annurev-arplant-050718-095851

Liu, D., Zhang, X., Li, Q., Xiao, Y., Zhang, G., Yin, W., Niu, M., Meng, W., Dong, N., Liu, J., et al. The U-box ubiquitin ligase TUD1 promotes brassinosteroid-induced GSK2 degradation in rice. Plant Commun. 2022:100450. https://doi.org/10.1016/j.xplc.2022.100450, preprint: not peer reviewed.

Liu J, Chen J, Zheng X, Wu F, Lin Q, Heng Y, Tian P, Cheng Z, Yu X, Zhou K, et al. GW5 acts in the brassinosteroid signaling pathway to regulate grain width and weight in rice. Nat Plants. 2017:**3**(5):17043. https://doi.org/10.1038/nplants.2017.43

Liu Q, Han R, Wu K, Zhang J, Ye Y, Wang S, Chen J, Pan Y, Li Q, Xu X, et al. G-protein betagamma subunits determine grain size through interaction with MADS-domain transcription factors in rice. Nat Commun. 2018:**9**(1): 852. https://doi.org/10.1038/s41467-018-03047-9

Ma XL, Zhang QY, Zhu QL, Liu W, Chen Y, Qiu R, Wang B, Yang ZF, Li HY, Lin YR, et al. A robust CRISPR/Cas9 system for convenient, high-efficiency multiplex genome editing in monocot and dicot plants. Mol Plant. 2015:**8**(8):1274–1284. https://doi.org/10.1016/j.molp.2015.04.007

Ngo QA, Baroux C, Guthörl D, Mozerov P, Collinge MA, Sundaresan V, Grossniklaus U. The armadillo repeat gene ZAK IXIK promotes Arabidopsis early embryo and endosperm development through a distinctive gametophytic maternal effect. Plant Cell. 2012:**24**(10): 4026–4043. https://doi.org/10.1105/tpc.112.102384

Rozas J, Ferrer-Mata A, Sanchez-DelBarrio JC, Guirao-Rico S, Librado P, Ramos-Onsins SE, Sanchez-Gracia A. DnaSP 6: DNA sequence polymorphism analysis of large data sets. Mol Biol Evol. 2017:**34**(12):3299–3302. https://doi.org/10.1093/molbev/msx248

Sakamoto T, Kitano H, Fujioka S. An E3 ubiquitin ligase, ERECT LEAF, functions in brassinosteroid signaling of rice. Plant Signal Behav. 2013:**8**(11):e27117. https://doi.org/10.4161/psb.27117

Sharma M, Singh A, Shankar A, Pandey A, Baranwal V, Kapoor S, Tyagi AK, Pandey GK. Comprehensive expression analysis of rice armadillo gene family during abiotic stress and development. DNA Res. 2014:**21**(3): 267–283. https://doi.org/10.1093/dnares/dst056

Shomura A, Izawa T, Ebana K, Ebitani T, Kanegae H, Konishi S, Yano M. Deletion in a gene associated with grain size increased yields during rice domestication. Nat Genet. 2008:**40**(8): 1023–1028. https://doi.org/10.1038/ng.169

Si L, Chen J, Huang X, Gong H, Luo J, Hou Q, Zhou T, Lu T, Zhu J, Shangguan Y, et al. OsSPL13 controls grain size in cultivated rice. Nat Genet. 2016:**48**(4): 447–456. https://doi.org/10.1038/ng.3518

Song XJ, Huang W, Shi M, Zhu MZ, Lin HX. A QTL for rice grain width and weight encodes a previously unknown RING-type E3 ubiquitin ligase. Nat. Genet. 2007:**39**(5): 623–630. https://doi.org/10.1038/ng2014

Sun S, Wang L, Mao H, Shao L, Li X, Xiao J, Ouyang Y, Zhang Q. A G-protein pathway determines grain size in rice. Nat Commun. 2018:**9**(1): 851. https://doi.org/10.1038/s41467-018-03141-y

Tewari R, Bailes E, Bunting KA, Coates JC. Armadillo-repeat protein functions: questions for little creatures. Trends Cell Biol. 2010:**20**(8): 470–481. https://doi.org/10.1016/j.tcb.2010.05.003

Tong HN, Chu CC. Functional specificities of brassinosteroid and potential utilization for crop improvement. Trends Plant Sci. 2018:**23**(11): 1016–1028. https://doi.org/10.1016/j.tplants.2018.08.007

Vogelmann K, Subert C, Danzberger N, Drechsel G, Bergler J, Kotur T, Burmester T, Hoth S. Plasma membrane-association of SAUL1-type plant U-box armadillo repeat proteins is conserved in land plants. Front Plant Sci. 2014:**5**:37. https://doi.org/10.3389/fpls.2014.00037

Wang A, Hou Q, Si L, Huang X, Luo J, Lu D, Zhu J, Shangguan Y, Miao J, Xie Y, et al. The PLATZ transcription factor GL6 affects grain length and number in rice. Plant Physiol. 2019:**180**(4): 2077–2090. https://doi.org/10.1104/pp.18.01574

Wang S, Li S, Liu Q, Wu K, Zhang J, Wang S, Wang Y, Chen X, Zhang Y, Gao C, et al. The OsSPL16-GW7 regulatory module determines grain shape and improves rice yield and quality. Nat Genet. 2015a:**47**(8): 949–954. https://doi.org/10.1038/ng.3352

Wang S, Wu K, Yuan Q, Liu X, Liu Z, Lin X, Zeng R, Zhu H, Dong G, Qian Q, et al. Control of grain size, shape, and quality by OsSPL16 in rice. Nat Genet. 2012:**44**(8): 950–954. https://doi.org/10.1038/ng.2327

Wang Y, Xiong G, Hu J, Jiang L, Yu H, Xu J, Fang Y, Zeng L, Xu E, Xu J, et al. Copy number variation at the GL7 locus contributes to grain size diversity in rice. Nat Genet. 2015b:**47**(8): 944–948. https://doi.org/10.1038/ng.3346

Weng J, Gu S, Wan X, Gao H, Guo T, Su N, Lei C, Zhang X, Cheng Z, Guo X, et al. Isolation and initial characterization of GW5, a major QTL associated with rice grain width and weight. Cell Res. 2008:**18**-(12): 1199–1209. https://doi.org/10.1038/cr.2008.307

Yang C, Shen W, He Y, Tian Z, Li J. OVATE Family protein 8 positively mediates brassinosteroid signaling through interacting with the GSK3-like kinase in rice. PLoS Genet. 2016:**12**(6): e1006118. https://doi.org/10.1371/journal.pgen.1006118

Ye H, Li L, Guo H, Yin Y. MYBL2 is a substrate of GSK3-like kinase BIN2 and acts as a corepressor of BES1 in brassinosteroid signaling pathway in Arabidopsis. Proc Natl Acad Sci USA. 2012:**109**(49):20142–20147. https://doi.org/10.1073/pnas.1205232109

Youn JH, Kim TW. Functional insights of plant GSK3-like kinases: multi-taskers in diverse cellular signal transduction pathways. Mol Plant. 2015:**8**(4):552–565. https://doi.org/10.1016/j.molp.2014.12.006

Yu J, Miao J, Zhang Z, Xiong H, Zhu X, Sun X, Pan Y, Liang Y, Zhang Q, Abdul Rehman RM, et al. Alternative splicing of OsLG3b controls grain length and yield in japonica rice. Plant Biotechnol J. 2018:**16**(9): 1667–1678. https://doi.org/10.1111/pbi.12903

Zeng LR, Qu S, Bordeos A, Yang C, Baraoidan M, Yan H, Xie Q, Nahm BH, Leung H, Wang GL. Spotted leaf11, a negative regulator of plant cell death and defense, encodes a U-box/armadillo repeat protein endowed with E3 ubiquitin ligase activity. Plant Cell. 2004:**16**(10): 2795–2808. https://doi.org/10.1105/tpc.104.025171

Zhao D, Zhang C, Li Q, Liu Q. Genetic control of grain appearance quality in rice. Biotechnol Adv. 2022:**60**:108014. https://doi.org/10.1016/j.biotechadv.2022.108014, November 2022, reprint: not peer reviewed.

Zhao DS, Li QF, Zhang CQ, Zhang C, Yang QQ, Pan LX, Ren XY, Lu J, Gu MH, Liu QQ. GS9 acts as a transcriptional activator to regulate rice grain shape and appearance quality. Nat Commun. 2018a:**9**(1): 1240. https://doi.org/10.1038/s41467-018-03616-y

Zhao H, Wang X, Jia Y, Minkenberg B, Wheatley M, Fan J, Jia MH, Famoso A, Edwards JD, Wamishe Y, et al. The rice blast resistance gene PTR encodes an atypical protein required for broad-spectrum disease resistance. Nat Commun. 2018b:**9**(1):2039. https://doi.org/10.1038/s41467-018-04369-4